Supplementary Information for

Spin-orbit-entangled state of Ba_2CaOsO_6 studied by O K-edge resonant inelastic X-ray scattering and Raman spectroscopy

J. Okamoto, G. Shibata, Yu. S. Ponosov, H. Hayashi, K. Yamaura, H. Y. Huang, A. Singh, C. T. Chen, A. Tanaka, S. V. Streltsov, D. J. Huang, and A. Fujimori

February 26, 2025

This SI file includes:

Supplementary Note 1. Phonon sidebands in RIXS spectra

In the low-energy O K-edge RIXS spectrum of Ba_2CaOsO_6 in Fig. 4(a), subpeaks separated by an interval of $\sim$ 80-meV are observed to accompany the quasi-elastic peak and the peaks at $E_{\rm loss} \simeq 0.4$ eV and 0.8 eV with intensities decreasing with energy. We attribute these sub-peaks to phonon replicas created by the simultaneous excitation of optical phonons. We investigated these multiplet excitation peaks and the phonons below energy loss of 1.5 eV referring to Živković $et\ al.$'s method [1]: Three multiplet excitation peaks and phonon side bands are fitted by Voigt functions and anti-Lorentzian functions, respectively. The background curve is a cubic function. Parameter values for the three multiplet excitations with Voigt functions are summarized in Supplementary Table 1: peak energy ω_0, Gaussian FWHM Γ_G, integrated intensity, and the FWHM ratio of the Lorentzian function against the Gaussian function Γ_L/Γ_G.

For the phonon satellites, the relative peak energies and intensities of the phonon satellites are shown in Supplementary Figures 1(a) and (b). The FWHMs of the anti-Lorentzian functions are set to 85 meV. The relative peak energies of the phonon satellites E_n^α(α = 1st, 2nd, and 3rd multiplet peaks) are well approximated by linear functions of phonon number n, $E_n^\alpha = nE_{\rm mode}$ with the energy of the optical phonon mode $E_{\rm mode}$ = 82$\pm$8 meV. From the intensity ratio of the phonon sidebands, the second harmonic intensities are $\sim 0.3 - 0.4$ of the first harmonic ones. Then, one can estimate the parameter of the electron-phonon coupling strength $M/\omega_0 \gtrsim 1$ referring to [2].

Supplementary Note 2. DFT calculations of phonon spectrum

In order to confirm the assignment of the phonon modes, we performed phonon calculations by the frozen phonons method [3] within the non-magnetic DFT. Os is a heavy transition-metal atom and, therefore, it is natural to include both strong electronic correlations (U) and the

spin-orbit coupling (SOC) via DFT+U+SOC approach. However, this method tends to stabilize magnetic solutions and cannot directly simulate the non-Kramers many-electron E_g states with zero projected total angular momentum $J^z_{eff} = 0$, which were proposed to be the ground state of Ba_2CaOsO_6 in case of cubic symmetry. Therefore, in Supplementary Figure 2 we present results of the non-magnetic phonon calculations [3]. The results of DFT+U+SOC approach shall be discussed below.

Phonon frequencies at the Γ-point were calculated by density functional perturbation theory (DFPT) in the DFT+U+SOC approach [4]. The same convergence criteria and parameter setup was used as in the frozen phonon calculations. On-site Hubbard repulsion parameter U and Hund's intra-atomic exchange ($J_{\rm H}$) were chosen to be $U = 3$ eV and $J_{\rm H} = 0.5$ eV, which are close to what is used for Os ions in the literature. The crystal structure was taken from [5]. We tested several combinations of magnetic orders [ferromagnetic and antiferromagnetic (AFM) of A-type] and directions of the total momentum ([001], [110], [111]) and obtained that the lowest total energy corresponds to $\rm Immm$ structure with Os AFM-A (ferromagnetic planes) and magnetic moments ordered in the ab-plane close [110] direction. In the relaxed structure OsO_6 octahedra are slightly elongated: four short 1.930 A and two long 1.945 A Os-O bonds.

Results of phonon calculations are shown in Supplementary Figure 2. The experimental spectrum agrees well with the oversimplified non-magnetic DFT calculation (except for the E_g mode). However, theoretical results for the cubic structure do not indicate any additional A_{1g} phonons at 720 cm^{-1} seen in the experiment.

Account of the spin-orbit coupling and Coulomb correlations by non-magnetic DFT+U+SOC ($U - J_{\rm H} = 2.5$ eV) calculations of phonon frequencies was performed only at the Γ-point using DFPT. It improves the position of the E_g band and yields $\omega_{A_{1g}} = 787$ cm^{-1} (experiment: 796.5 cm^{-1}), $\omega_{E_g} = 525$ cm^{-1} (experiment: 495 cm^{-1}), $\omega_{T_{2g}} = 355$ cm^{-1} (experiment: 375 cm^{-1}), and $\omega_{T_{2g}} = 105$ cm^{-1} (experiment: 101.5 cm^{-1}). However, as explained above the

undistorted cubic structure turns out unstable in GGA+U+SOC therefore there appear imaginary acoustic and low-frequency optical modes. The DFPT calculations demonstrate that the E_g phonon mode splits, but the splitting does not exceed 30 cm^{-1}, so one cannot attribute two experimentally observed peaks at 495 and 720 cm^{-1} to E_g phonon split due to the Jahn-Teller effect. Nevertheless, experimental peak at 495 cm^{-1} is extremely broad and therefore the splitting of this line can remain unnoticed. Unexpected appearance of the extra A_{1g} mode at 720 cm^{-1} can be due to a non-negligible disorder in B sites. Indeed folding of the Brillouin zone, e.g. when $U \to \Gamma$, would lead to the appearance of an additional (weak) mode at $\sim$90 meV.

Supplementary References

[1] I. Živković, *et al.*, Dynamic Jahn-Teller effect in the strong spin-orbit coupling regime, *Nat. Commun.* **15**, 8587 (2024).

[2] L. J. P. Ament, M. van Veenendaal, J. van den Brink, Determining the electron-phonon coupling strength from resonant inelastic X-ray scattering at transition metal L-edges, *Europhys. Lett.* **95**, 27008 (2011).

[3] A. Togo, First-principles phonon calculations with phonopy and phono3py, *J. Phys. Soc. Jpn.* **92**, 012001 (2023).

[4] S. L. Dudarev, S. Y. Savrasov, C. J. Humphreys, A. P. Sutton, Electron-energy-loss spectra and the structural stability of nickel oxide: An LSDA+U study, *Phys. Rev. B* **57**, 1505-1509 (1998).

[5] K. Yamamura, M. Wakeshima, Y. Hinatsu, Structural phase transition and magnetic properties of double perovskites Ba_2CaMO_6 (M = W, Re, Os), *J. Solid State Chem.* **179**, 605-612 (2006).

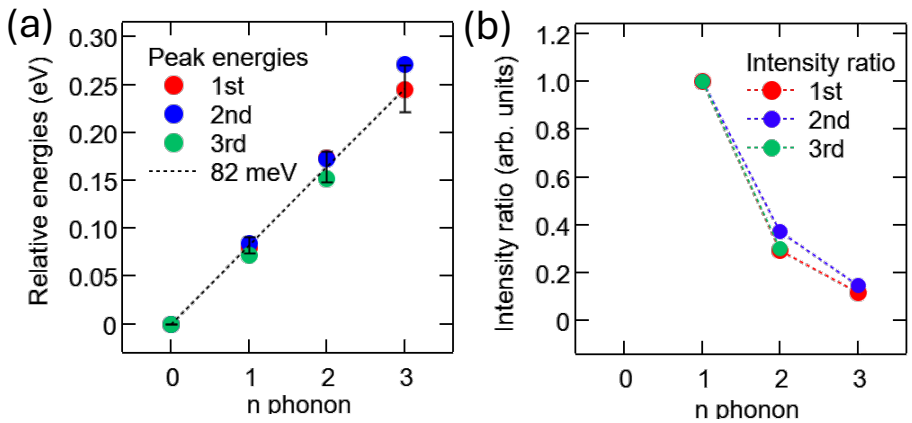

Supplementary Figure 1: Line-shape analysis of the phonon side bands in the RIXS spectrum in Fig. 4(a), (a) Relative energies of the phonon satellites. (b) Relative intensities of the phonon satellites. 1st: $J_{\text{eff}} = 2 \rightarrow 2$ multiplet excitation, 2nd: $J_{\text{eff}} = 2 \rightarrow 0, 1$ excitation, 3rd: $J_{\text{eff}} = 2 \rightarrow 2$ excitation.

Supplementary Table 1: Parameter values of the Voigt functions for the three multiplet excitation peaks.

Parameter	1st	2nd	3rd
Peak energy ω_0 (eV)	0.0	0.397	0.788
FWHM of Gaussian Γ_G (meV)	32.4	45.2	45.0
Integrated intensity (arb. units)	216.6	145.1	36.0
FWHM ratio Γ_L/Γ_G	0.85	0.54	1.28

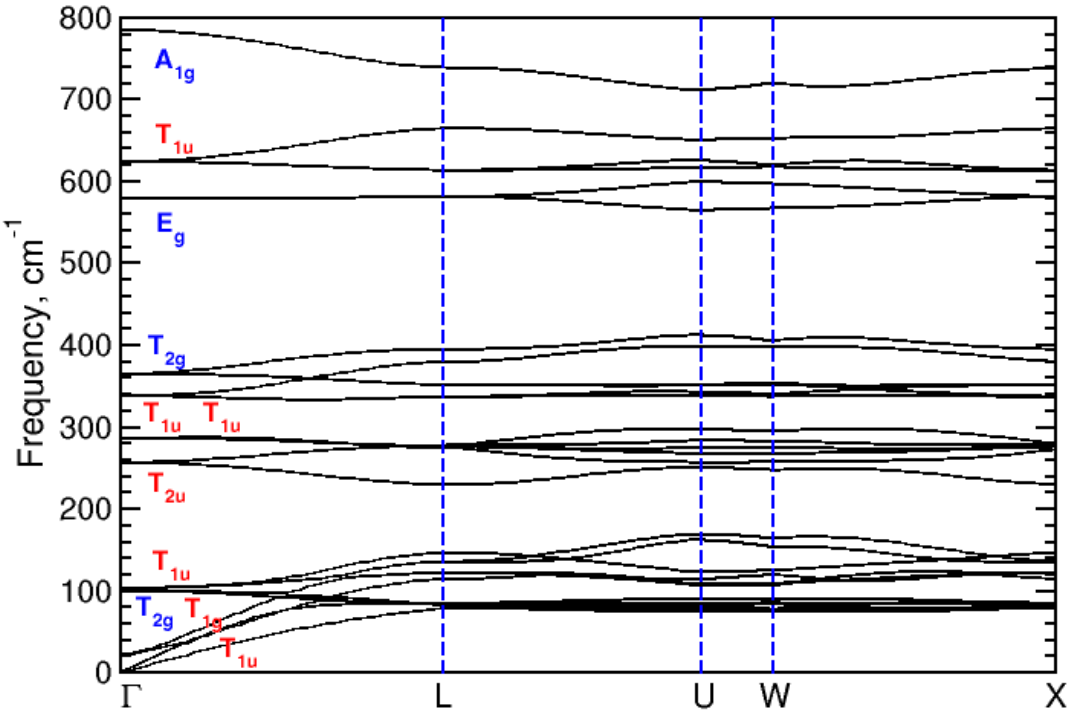

Supplementary Figure 2: Phonon dispersions (together with characters) as calculated by non-magnetic DFT.

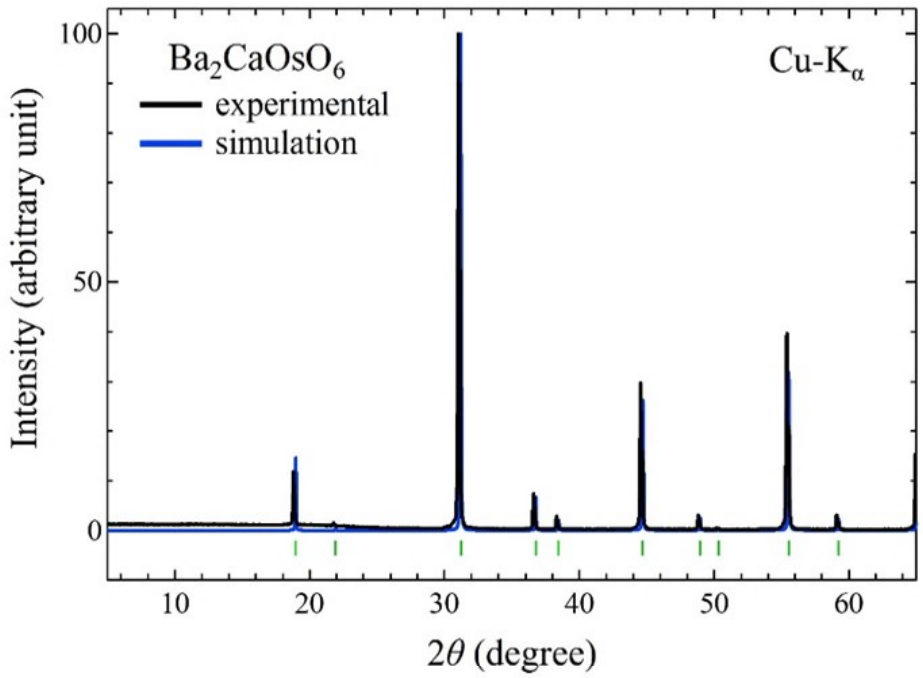

Supplementary Figure 3: Powder X-ray diffraction of the polycrystalline Ba_2CaOsO_6 sample.